JOURNAL OF CATALYSIS 72, 218–235 (1981)

The Characterisation of Carbon-Fibre-Paper-Supported Platinum and Platinum–Ruthenium Catalysts Using Temperature-Programmed Reduction and Cyclic Voltammetry

T. MAHMOOD AND J. O. WILLIAMS

Edward Davies Chemical Laboratories, University College of Wales, Aberystwyth, Dyfed, Wales

AND

R. MILES AND B. D. MCNICOL

Shell Research Ltd., Thornton Research Centre, P.O. Box 1, Chester CH1 3SH, England

Received November 25, 1980; revised August 13, 1981

Temperature-programmed reduction (TPR) and cyclic voltammetry have been used to investigate Pt and Pt–Ru dispersed catalysts unsupported and supported on conducting carbon at various stages of the catalyst preparation. Differences in the TPR profiles and the corresponding uptake of H_2 by unsupported and supported $Pt(NH_3)_2(NO_2)_2$ dried from HNO_3 solution at 120°C are attributed to an interaction via ligand exchange between the nitrato-substituted Pt complex and nucleophilic surface groups formed on the carbon support by the action of HNO_3. A similar interaction was observed for carbon-supported Ru salts prepared from $RuNO(NO_3)_x$. Support interactions present after the drying stage led to an enhanced catalyst dispersion and to the elimination of the original interaction after activation in air at 300°C. Bimetallic Pt–Ru catalysts display reducibilities in TPR intermediate between those observed for the pure components in both unsupported and supported forms. The influence of the carbon support is absent after activation in air. At 300°C, activation produces a high bimetallic dispersion (90 $m^2 g^{-1}$) whereas activation at 400°C leads to more perfect alloy formation and consequently to an increased intrinsic activity as an electrocatalyst for methanol oxidation at the expense of a reduced dispersion (54 $m^2 g^{-1}$). Cathodic processes at 0.1–0.4 V (vs RHE) during the initial linear potential sweep, corresponding to oxide reduction, are observed for air-activated Pt and Pt–Ru catalysts. Electrochemical reduction of oxide species in this way is analogous to the characteristic processes observed in TPR except that initial cathodic reduction extends ca.4 atomic layers into the oxide particles. Our conclusions concerning air-activated Pt catalysts, largely composed of PtO_2, are in essential agreement with similar studies of oxide layers formed electrochemically on smooth Pt electrodes.

INTRODUCTION

Catalyst characterisation necessitates detailed analysis of the chemical state at each stage of preparation, for example, after impregnation, drying, calcination, and reduction (*1*, *2*). In bimetallic catalysts, for instance, interactions may occur between the two metallic components at each stage of the preparation (*3*). Also, the degree of interaction with the support can be strongly influenced by the preparative conditions (*4*). A further factor that can modify the surface composition of mixed metal catalysts is surface enrichment in that component which lowers the surface free energy of catalyst particles (*5*). Finally, the gaseous atmosphere utilised in thermal treatment of alloy catalysts may induce surface segregation of the metallic components via selective chemisorption (*6*, *7*). Recently, Jenkins and co-workers (*8*, *9*) demonstrated that the technique of Temperature-Programmed Reduction (TPR) can provide information on the form of oxidic species present in catalysts. During TPR analysis, the catalyst sample is cooled under an inert gas flow (typically nitrogen) to a sufficiently

0021-9517/81/120218-18$02.00/0

low temperature, e.g., −196°C, such that no significant reaction occurs on subsequent exposure to a hydrogen/inert-carrier gas flow. The temperature of the sample is then increased at a linear rate resulting in a characteristic reduction, which is monitored as consumption of hydrogen as a function of temperature. Such factors as linear heating rate, sample size, hydrogen partial pressure, and flow rate can influence the form of the reduction process and hence are maintained constant throughout a series of experiments. The technique is relatively sensitive compared with many other bulk methods, being capable of detecting reducible species requiring only 10^{-8} mole hydrogen for complete reduction. It has been shown that alloying (*10*), metal-support interaction (*11, 12*), and spillover of hydrogen onto oxide supports (*13*) can be detected by this method.

The experimental techniques of Linear Sweep Voltammetry (LSV) and Cyclic Voltammetry (CV) have long been employed in electrochemistry to study adsorption/desorption processes involving charge transfer at electrode surfaces (*14, 15*). In particular, CV has enabled the surface compositions of smooth metal alloys (*16*) and mixed metal catalysts (*17*) to be determined from an examination of characteristic oxidation/reduction processes in aqueous acid electrolytes. Also, surface areas of platinum catalysts can be quantitatively estimated from the degree of hydrogen electrosorption (*18, 19*). In LSV or CV the electrode potential is scanned at a constant rate between two potential limits, either once or cyclically following a triangular waveform, and the corresponding currents are measured. An analogy can be drawn between LSV in a cathodic direction, whereby a linearly decreasing potential induces the electrochemical reduction of surface oxides, and TPR, whereby chemical reduction of bulk and surface oxides is achieved under conditions of linearly increasing temperature. In the case of TPR, the reaction is favoured thermodynamically owing to a negative free energy change but is limited kinetically depending on temperature, whilst during LSV the potential and hence free energy of the electrode is varied such that the reduction process ensues at a characteristic potential. Clearly, the electrode material under study must be stable towards dissolution in the surrounding electrolyte as well as electrically conducting. Generally, noble metal catalysts supported on carbon or graphite are amenable to electrochemical study. By judicious application of both TPR and CV, the bulk and surface properties of such catalysts can be determined after each stage of the preparation.

Alloy formation in platinum–ruthenium catalysts, active for methanol electrooxidation, has previously been identified using TPR and CV (*20*). Also, the variation in surface composition with different types of thermal activation, as determined by CV, for supported Pt–Ru catalysts has been highlighted (*7*). A pyrographite-coated carbon fibre (PGCF) paper is used as the support and recently some attention has been given to the possible interaction that can occur between Pt compounds and surface groups on the PGCF paper since it is believed that this interaction plays a role in generating the high electrocatalytic activity of such catalysts (*21*).

In this paper we present some results on the characterisation of Pt and Pt–Ru catalysts both unsupported and supported on PGCF paper using TPR and CV. The procedure used was to evaluate the state of the catalyst after the stages of impregnation/drying and calcination (activation in air) in order to obtain information about the nature of the catalyst and the interaction between catalyst and support.

EXPERIMENTAL

Catalyst Preparation

(*a*) *Unsupported catalysts.* Three different preparations of unsupported Pt catalysts were considered. The first preparation utilised platinum diammine dinitrite,

$Pt(NH_3)_2(NO_2)_2$ (Johnson–Matthey Chemicals, Ltd.) as supplied, the second was obtained by evaporation of an aqueous solution of $Pt(NH_3)_2(NO_2)_2$ to dryness and the third by evaporation of a solution of $Pt(NH_3)_2(NO_2)_2$ in 3*M* HNO_3. After final drying in air at 120°C for 16 hr, the catalysts were calcined in flowing air by heating to 300°C at a rate of 20°C min^{-1} and maintained at this temperature for 1 hr. Mixed metal catalysts containing Ru and monometallic Ru catalysts were prepared from a HNO_3 solution of ruthenium nitrosyl nitrate, $RuNO(NO_3)_x$ (Johnson–Matthey Chemicals, Ltd.) using the same procedure as outlined above. PtO_2 and RuO_2 (Engelhard Industries, Ltd.), prepared by the Adams method, were used without further treatment.

(*b*) *Supported catalysts.* A cellulose-based carbon fibre paper support (Stonehart Associates, Inc.) was covered with a layer of pyrographite by pyrolysis of a 5% CH_4/95% N_2 mixture at 1250°C for 4 hr prior to use. The resulting PGCF paper possessed a surface area of <1 m^2 g^{-1} (N_2, BET) a thickness of 250 μm and an area density of 20 mg cm^{-2}. The support was impregnated with a solution of $Pt(NH_3)_2(NO_2)_2$ in H_2O or 3*M* HNO_3. For Ru-containing catalysts, $RuNO(NO_3)_x$ in 3*M* HNO_3 was used. In all cases, the impregnating solution contained 5 mg total metal per cubic centimetre. Impregnation was carried out by dropwise addition under an infrared lamp to give metal loadings of about 0.5–1.0 mg cm^{-2} and subsequent drying and calcination in air followed the same procedure as described for unsupported catalysts.

Catalyst Characterisation

(*a*) *Temperature-Programmed Reduction (TPR).* The experimental apparatus used for the TPR measurements consisted of a modified Perkin–Elmer Model 212D Sorptometer in which the reducing gas was passed through one arm of a thermal conductivity cell, thence through a silica U-tube reactor and finally via a cold trap (at −78°C) back through the other arm of the thermal conductivity cell. For the present study the initial reactor temperature was extended to −196°C, since it had been found earlier (*22*) that with carbon-fibre-paper-supported Pt catalysts, calcination resulted in oxidised species capable of reduction by H_2 at temperatures below ambient. The heating rate throughout was 6°C min^{-1} and the reducing gas composition was 5%/95%: H_2/N_2 (v/v). A gas flow rate of 900 cm^3 min^{-1} was used at absolute pressures of 1 bar and calibration was achieved by the injection of a known volume (0.237 cm^3) of pure H_2 into the inlet stream at the end of each run. Sample sizes used in TPR ranged between 0.2 and 2 mg metal (typically 0.7 mg).

(*b*) *Cyclic Voltammetry (CV).* An identical experimental arrangement to that described in an earlier paper (*7*) was used. A three-compartment electrochemical cell containing 3*M* H_2SO_4 (BDH Chemicals Ltd), preelectrolysed for 7 days to eliminate organic impurities, was maintained at 25°C for all experiments. Electrochemical reduction of oxidic species was initially monitored by sweeping the electrode potential cathodically from +0.7 V (vs RHE) to 0.0 V at a linear potential sweep rate of 2 mV sec^{-1}. Subsequent cyclic voltammograms of the reduced catalyst were recorded between the potential limits 0.0 V and +1.6 V for Pt catalysts (+1.4 V in the case of Pt–Ru catalysts) at a sweep rate of 50 mV sec^{-1}. Metal surface areas were determined electrochemically by integration of the anodic current passed (excluding double-layer charging) in the potential range 0.0–0.4 V corresponding to the discharge of adsorbed H atoms. Complete coverage of the Pt surface was assumed to require a specific charge of 210 μC cm^{-2} (*23, 24*).

(*c*) *Chemical analysis.* Elemental analysis for Pt and Ru was carried out by atomic absorption spectrophotometry (AAS) using a Perkin-Elmer Model 560

spectrophotometer. Samples were extracted by boiling in a 3 : 1 HCl/HNO_3 mixture and the resulting solution was made up to a known volume in 10%v HCl. Interelemental interference was minimised by the addition of 5000 ppm uranium (as uranyl nitrate) to the final solution.

RESULTS AND DISCUSSION

(*a*) *Monometallic Pt Catalysts*

Significant differences were observed in the TPR profiles of unsupported Pt salts dried from aqueous and HNO_3 solution at 120°C (Fig. 1a). Reduction maxima occurred at 169 and 144°C respectively and furthermore the total uptake of hydrogen differed considerably as indicated in Table 1. Stoichiometric reduction of $Pt(NH_3)_2(NO_2)_2$ results in the consumption of 7 moles H_2 per g-atom Pt as follows:

$$Pt(NH_3)_2(NO_2)_2 + 7H_2 \rightarrow Pt + 4H_2O + 4NH_3. \quad (1)$$

Experimentally, $Pt(NH_3)_2(NO_2)_2$, as received, is found to consume 7.0 ± 0.5 moles H_2 at a temperature centred at 166°C. A corresponding value of $H_2/Pt = 12.7$ for HNO_3-dried $Pt(NH_3)_2(NO_2)$ indicated that a transformation of the original compound had taken place through interaction with HNO_3. In concentrated HNO_3, it is known (*25*) that replacement of the NH_3 ligands takes place to form $[Pt(NO_2)_2(NO_3)_2]^{2-}$. AAS analysis of the dried salts confirmed that partial ligand substitution had occurred. In 3*M* HNO_3, ligand exchange between NH_3 and H_2O is also possible resulting in a compound of average composition $[Pt(NO_3)_xL_{(2-x)}(NO_2)_2]^{x-} \cdot xH_3O^+$, where $L = NH_3$ or H_2O. Solving for x on the basis of results from TPR and elemental analysis, respectively, yields values of 0.44 and 0.30 for the sample dried from aqueous solution, and 1.57 and 1.17 for that prepared from 3*M* HNO_3 solution. Hence, in the latter sample approximately 70% substitution of NH_3 by NO_3^- has taken place, thus explaining the difference in the TPR characteristics of these two samples.

Changes in the nature of the dried salts arise on drying the solutions onto carbon fibre, especially in the case of $Pt(NH_3)_2(NO_2)_2$ dissolved in HNO_3. The TPR profiles shift to higher temperature by 11 and 66°C respectively for the samples prepared from aqueous and HNO_3 solutions (Fig. 1b). The large shift of the TPR profile in the latter case is associated with a 44% decrease in the uptake of H_2 (see Table 1), indicating the presence of a significant interaction with the carbon support even at the drying stage of catalyst preparation. In contrast to aqueous impregnation, HNO_3 is able to generate acidic surface oxides (*21*) especially since the acid concentration progressively increases during evaporation of H_2O from the solution. The acidic surface oxides, e.g., carboxylic acid groups, are strong nucleophiles and so are able to substitute ammine ligands of the Pt(II) complex resulting in an anchored structure. Reduction during TPR brings about dissociation of the surface complex and reduction of the nitrito groups consuming seven molecules of H_2 per Pt atom. On activation, the surface interaction in the supported Pt catalyst prepared from HNO_3 solution leads to an increased Pt metal dispersion and consequent higher catalytic activity compared with a Pt catalyst prepared by aqueous impregnation, as described below.

After activation in air at 300°C, the unsupported catalysts prepared from $Pt(NH_3)_2(NO_2)_2$, as supplied, and from the aqueous solution of the salt displayed no significant reduction process during TPR. X-Ray powder diffraction confirmed that the catalyst after activation contained only metallic Pt as the identifiable crystalline phase. It appears that calcination of $Pt(NH_3)_2(NO_2)_2$ leads to a rapid exothermic oxidation of the NH_3 ligands leading to a sudden rise in temperature and the resultant ignition of the salt, yielding a Pt sponge. In contrast, the unsupported sample prepared from HNO_3 solution displayed

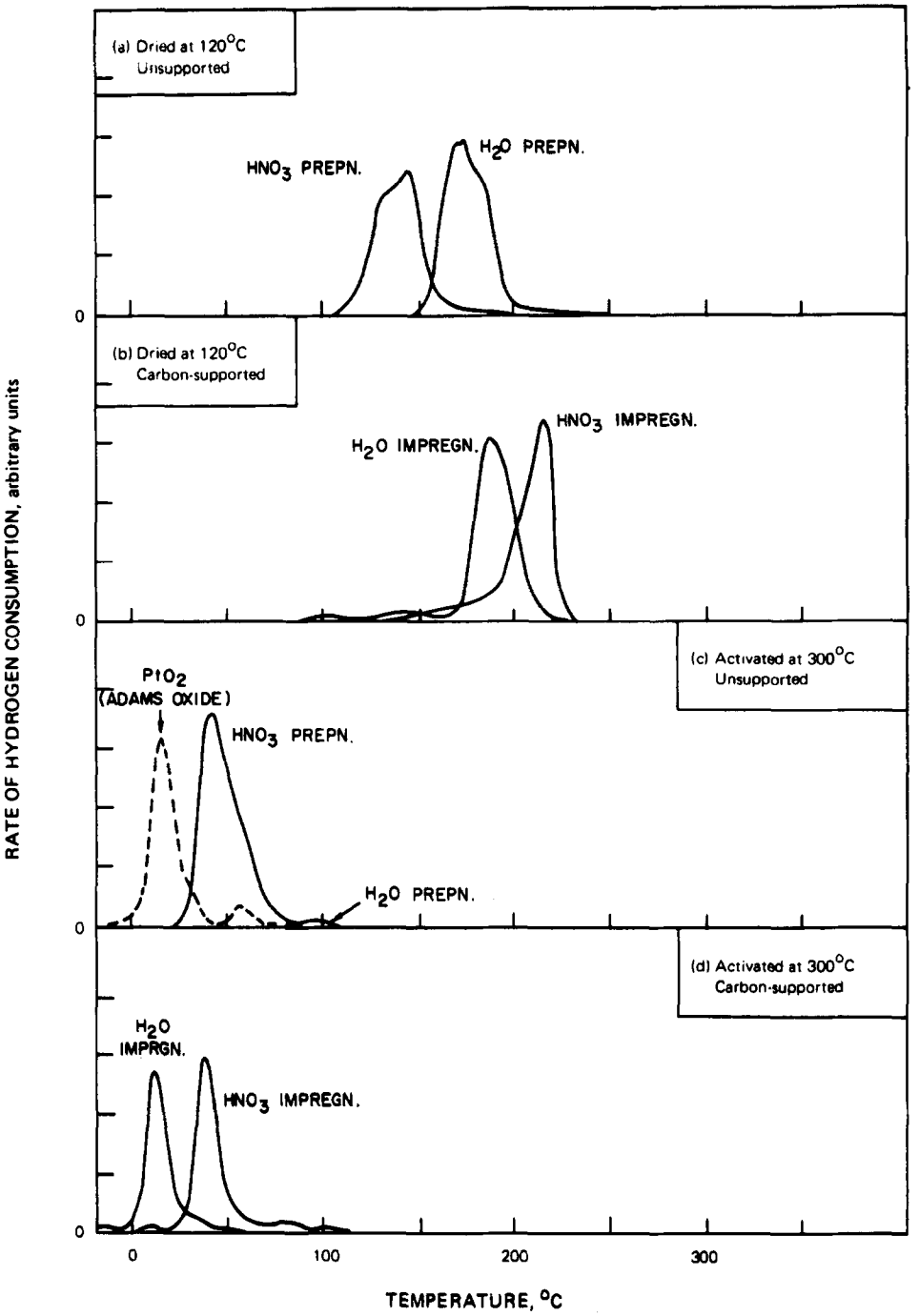

FIG. 1. TPR characteristics of Pt monometallic catalysts.

a well-defined reduction peak during TPR (Fig. 1c). Clearly, reductive decomposition does not occur during calcination in this case owing to substitution of NH_3 by NO_3^- in the Pt complex lowering the exothermicity of the reaction. The quantitative uptake of H_2 during TPR analysis corresponded to the reduction stoichiometry;

TABLE 1

Hydrogen Consumption during TPR of Pt–Ru Catalysts

Impregnating solution	Pretreatment (in air)	Unsupported catalyst		Carbon-supported catalyst	
		Bulk composition at.% Pt : at.% Ru	Total hydrogen consumption $\left[\frac{\text{mole } H_2}{\text{(g-atom total metal)}}\right]$	Bulk composition at.% Pt : at.% Ru	Total hydrogen consumption $\left[\frac{\text{mole } H_2}{\text{(g-atom total metal)}}\right]$
$Pt(NH_3)_2(NO_2)_2$ in H_2O		100 : 0	9.33	100 : 0	7.54
$Pt(NH_3)_2(NO_2)_2$ in 3*M* HNO_3		100 : 0	12.72	100 : 0	7.08
$Pt(NH_3)_2(NO_2)_2$ and	Dried at 120°C	79 : 21	11.59	85 : 15	7.43
$RuNO(NO_3)x$ in 3*M* HNO_3		57 : 43	10.62	64 : 36	9.40
$RuNO(NO_3)x$ in 3*M* HNO_3		0 : 100	—	0 : 100	16.3
$Pt(NH_3)_2(NO_2)_2$ in H_2O	Dried at 120°C	100 : 0	0.02	100 : 0	1.73
$Pt(NH_3)_2(NO_2)_2$ in 3*M* HNO_3	followed by	100 : 0	2.43	100 : 0	2.14
$Pt(NH_3)_2(NO_2)_2$ and	activation	81 : 19	4.41	87 : 13	2.27
$RuNO(NO_3)x$ in 3*M* HNO_3	at 300°C	57 : 43	—	74 : 26	5.30
$RuNO(NO_3)x$ in 3*M* HNO_3		0 : 100	—	0 : 100	10.7

$$PtO_2 + 2H_2 \rightarrow Pt + 2H_2O. \quad (2)$$

The temperature of the reduction maximum (45°C), whilst considerably higher than that previously observed for PtO, was found to occur in a similar temperature region to that of unsupported PtO_2 prepared by the Adams method. For the supported catalyst prepared by aqueous impregnation, no ignition took place on calcination since the sample possessed a reduction profile during TPR characteristic of PtO_2, both in temperature and stoichiometry (Fig. 1d and Table 1). Evidently, the carbon support assists in the dissipation of the heat of reaction preventing thermal dissociation of the metal oxide through localised heating.

Electrochemical measurement of monometallic Pt catalysts is restricted to an investigation of the activated catalysts since dried samples are unstable towards dissolution in the H_2SO_4 electrolyte. A voltammogram of an activated Pt catalyst prepared by HNO_3 impregnation is shown in Fig. 2. An initial potential sweep from +0.7 V, in a cathodic direction to 0.0 V, was performed at a relatively slow linear rate of 2 mV sec^{-1} inducing electrochemical reduction of Pt oxides, in acid electrolyte according to, for example, the following reactions (*26*);

$$PtO_2 + 4H^+ + 4e^- = Pt + 2H_2O, \quad E^\circ = 0.50 \text{ V},^1 \quad (3)$$

$$PtO + 2H^+ + 2e^- = Pt + H_2O, \quad E^\circ = 0.98 \text{ V}. \quad (4)$$

Other stepwise processes can also be envisaged, for example

$$PtO_2 + 2H^+ + 2e^- = Pt(OH)_2, \quad E^\circ = 1.1 \text{ V}, \quad (5)$$

$$Pt(OH)_2 + 2H^+ + 2e^- = Pt + 2H_2O, \quad E^\circ = 0.98 \text{ V}. \quad (6)$$

In these and all other cases the standard electrochemical potential (E°) is sufficiently anodic that oxide reduction to metallic Pt is theoretically achieved during the initial slow cathodic sweep to 0.0 V. Inspection of Fig. 2 shows that a narrow and intense cathodic peak superimposed on a lesser broadened peak occurs at a potential of +0.38 V during the initial sweep, the form of which is dependent on the preparative method. The single peak corresponding to oxide reduction is analogous to that observed by TPR, where chemical reduction of the oxide occurs. Similar observations have also been recently made using supported Pt catalysts prepared both by impregnation and ion-exchange from $Pt(NH_3)_4(OH)_2$ (*22*).

The first complete cycle of the voltammogram (Fig. 2) shows features typical of Pt metal. Integration of the charge associated with hydrogen desorption (q_H) enabled quantitative estimates to be made of the specific Pt surface area (*23, 24*). Catalysts prepared by impregnation from HNO_3 solution yielded a relatively high surface area; i.e., 39.5 ± 3.9 $m^2\ g^{-1}$ (average of 5 samples), compared with a value of 22.4 ± 1.3 $m^2\ g^{-1}$ (average of 5 samples) for catalysts prepared from aqueous solution.

A direct relationship was found between the charge associated with the initial oxide reduction, q_{ox}, observed during the initial cathodic sweep from 0.7 V and the Pt surface area calculated from q_H as shown in Fig. 3. Since TPR had previously shown that the samples are largely composed of PtO_2, it was concluded from inspection of the ratio q_{ox}/q_H that electrochemical reduction, under the conditions of the experiment, extends on average 4.2 ± 0.7 atomic layers into the oxide particles irrespective of particle size. No systematic electrochemical studies of dispersed Pt oxides have previously been reported; however, many investigations have been made of oxide formation and reduction on smooth Pt metal. Under conditions of high anodic potential in acid electrolyte, Pt metal forms a mixed oxide film, as shown by direct chemical analysis (*27*). Shibata and Sumino (*28*) prepared Pt oxide films by anodic oxidation at 2.07–2.22 V, which they showed by cath-

[1] Calculated from free energy data.

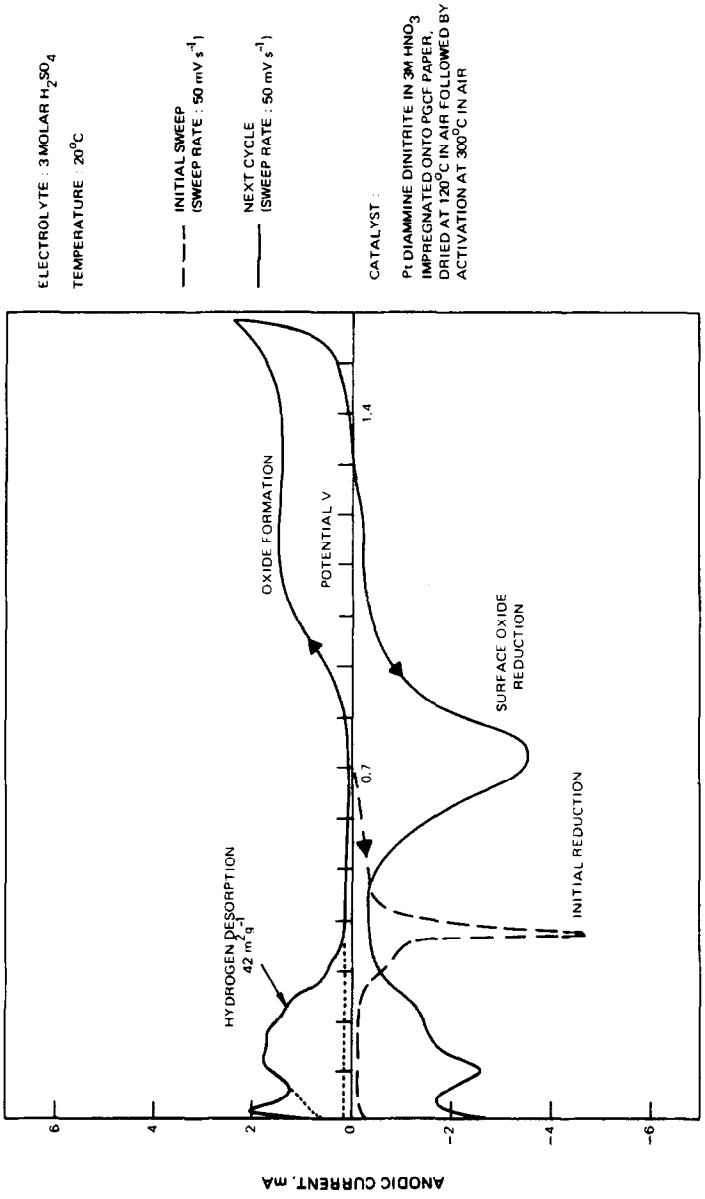

FIG. 2. Cyclic voltammogram of a monometallic Pt catalyst supported on carbon fibre paper.

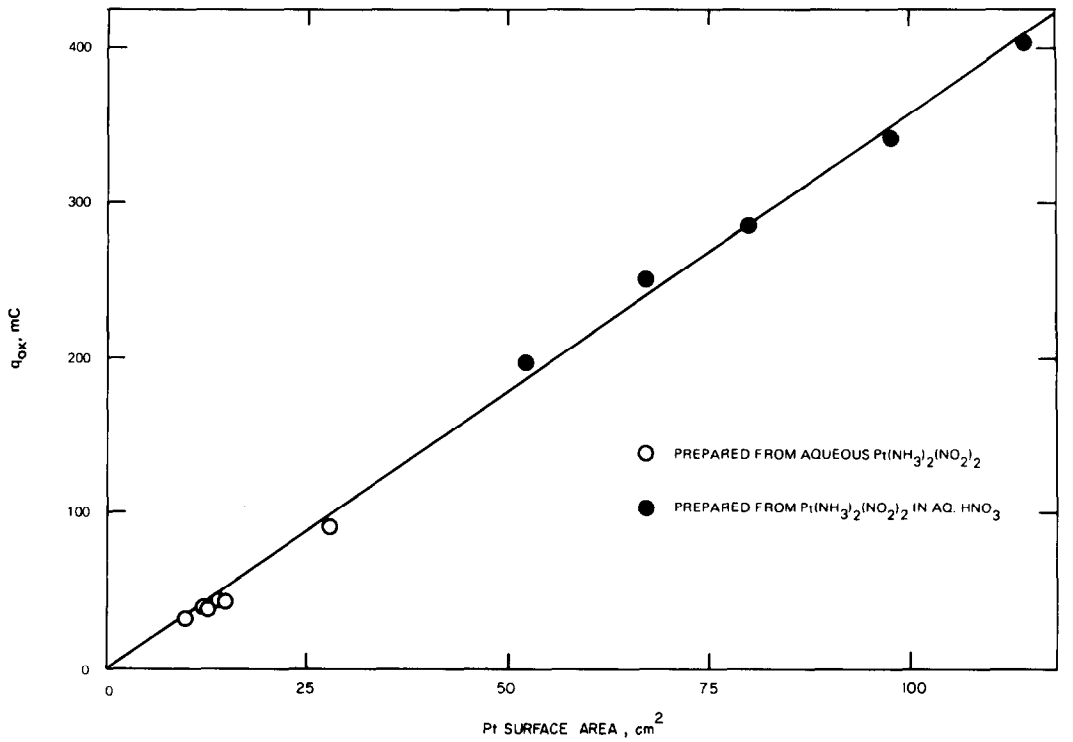

FIG. 3. Relationship between the coulombic charge associated with electrochemical reduction of Pt oxide catalysts and Pt surface area.

odic reduction to comprise two distinct layers; these were an α-layer corresponding to a superficial monolayer oxide which reduced at ca. +0.7 V and a β-layer which reduced at ca. +0.3 V and possessed properties of a multilayer oxide. In a later paper, Shibata (*29*) used electron diffraction methods to analyse the subsurface "phase oxide" and showed it to consist of poorly crystalline PtO_2. Thus it appears valid to compare the electrochemical properties of dispersed Pt oxides reported here with the properties of anodically formed multilayer oxides on smooth Pt. More recent studies (*30, 31*) have shown that reduction of the β-phase oxide starts at +0.35 V and is assisted by strongly adsorbed H atoms which discharge to form protons and migrate across the reduced α-film under the influence of the high electric field. On reaching the β-oxide layer the protons combine with O_2^- ions. Gileadi *et al.* (*32*) consider proton migration to be the rate-determining step for the overall reduction of the β-oxide. Extraction of oxygen species from the PtO_2 lattice by a place-exchange mechanism must however be energetically unfavourable. Angerstein-Kozlowska *et al.* (*33*), for instance, have explained the stabilisation of noble metal oxides by cations in terms of a diminished tendency for place-exchange to occur. Thus, from our results, place-exchange of oxygen species by Pt atoms appears to be restricted, on average, to the first few atomic layers of the Pt subsurface. We intend shortly to report an extensive study into the electrochemical reduction of dispersed Pt oxides.

(*b*) *Monometallic Ru Catalysts*

The unsupported ruthenium nitrosyl nitrate salt after drying at 120°C reduced during TPR in a broadened peak with a maximum at 261°C extending to higher

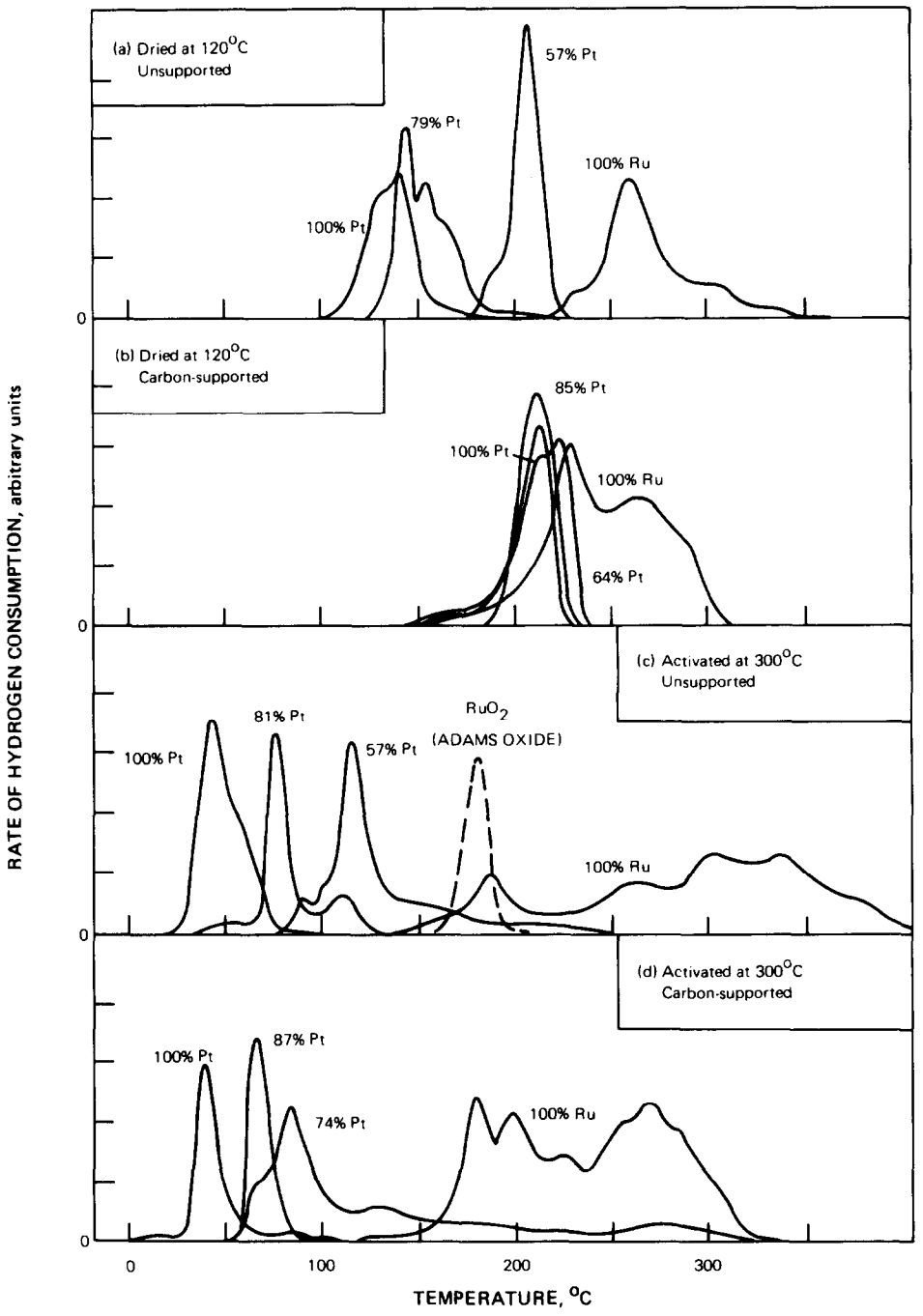

FIG. 4. TPR characteristics of Pt–Ru bimetallic catalysts.

temperatures (Fig. 4a). In comparison, the carbon-supported ruthenium compound reduced in a similar temperature range exhibiting two distinct peaks at 230 and 265°C (Fig. 4b). Incomplete extraction of the reduced Ru metal, which tended to form a Ru "mirror" over the internal surface of the silica reaction tube, prevented accurate es-

timates of the stoichiometry of the reaction with H_2 during TPR. The appearance of a relatively narrow peak at lower temperatures accounting for approximately 20% of the total H_2 consumption in the supported sample does, however, indicate that changes in chemical composition are induced by the support. Since the nitrosyl ruthenium complex is impregnated from HNO_3 solution, it may be expected that acidic surface groups, formed at the carbon surface during drying, influence the chemical composition of the dried complex.

Various studies of nitrato-substituted nitrosylruthenium (III) complexes in aqueous HNO_3 have been reported in the literature (*34–37*). Ligand substitution in the octahedral nitrosylruthenium (III) complex in HNO_3 solution gives rise to neutral, anionic, and cationic complexes of general formula $[RuNO(NO_3)_y(H_2O)_{5-y}]$ depending on acid concentration (*34*).

It thus appears that, as in the case of the dried Pt salts, a ligand- or ion-exchange process occurs at surfaces possessing acidic carbon groups modifying the composition of the dried Ru compounds. Interactions of this kind may favour cationic groups such as $[RuNO(NO_3)_2(H_2O)_3]^+$, $[RuNO(NO_3)(H_2O)_4]^{2+}$, and especially $Ru_4(OH)_{12}^{4+}$, which accounts for 80% of the total Ru in 10*M* HNO_3 under certain conditions (*37*). However, measurement of the amount of H_2 consumed during TPR (Table 1) suggests that the trinitrato-complex is the major component in the dried supported Ru salt according to the following stoichiometry;

$$RuNO(NO_3)_3(H_2O)_2 + 16H_2 \rightarrow Ru + 4NH_3 + 12H_2O, \quad (7)$$

For which reaction, $H_2/Ru = 16$.

Upon air activation at 300°C, the unsupported Ru catalyst reduced over a wide temperature range during TPR, exhibiting a narrow peak of low intensity at 185°C and three broader components at 260, 303, and 335°C (Fig. 4c). The supported catalyst also underwent reduction in stages, displaying peaks at 180, 198, 225, and 265°C. In the latter case the hydrogen consumption corresponded to $H_2/Ru = 10.7$ (Table 1) showing that incomplete decomposition to metal oxide occurs in air at 300°C. Confirmation of this finding was provided by Differential Thermal Analysis which showed that the exothermic reaction in air reaches a maximum at 400°C. Identical PGCF paper-supported samples were therefore activated in air at the higher temperature of 400°C in order to convert the material more fully into the oxide. TPR of the Ru catalyst activated at 400°C indeed showed a single reduction peak at 195°C, accounting for a lower uptake of H_2 (Fig. 5b). Thus the two reduction peaks previously observed at 220 and 265°C during TPR analysis of the 300°C activated sample probably arise from the undecomposed nitrato Ru component. Further TPR experiments using RuO_2 Adams oxide indicated that the reduction peak at 180–200°C arises from the reduction of an RuO_2 species (Figs. 4c or 5a).

(*c*) *Bimetallic Pt–Ru Catalysts*

Mixed impregnation of Pt and Ru salts results in dried compounds, which in TPR display reducibilities intermediate in character between those observed for the pure components, both for the unsupported (Fig. 4a) and supported cases (Fig. 4b). Generally, the bimetallic mixture shows only a single reduction peak. A plot of the temperature of the reduction maximum (or temperature corresponding to 50% reaction) against the atomic ratio of Pt and Ru as shown in Fig. 6 is approximately linear between the limits of the pure components except for a slight deviation at low Ru fractions. Clearly, efficient mixing of the two metallic fractions has taken place during impregnation such that reduction of the less reducible Ru complex is catalysed by neighbouring prereduced Pt atoms, resulting in a single overall process. Superimposed on this effect we see an influence of the carbon support as described earlier for

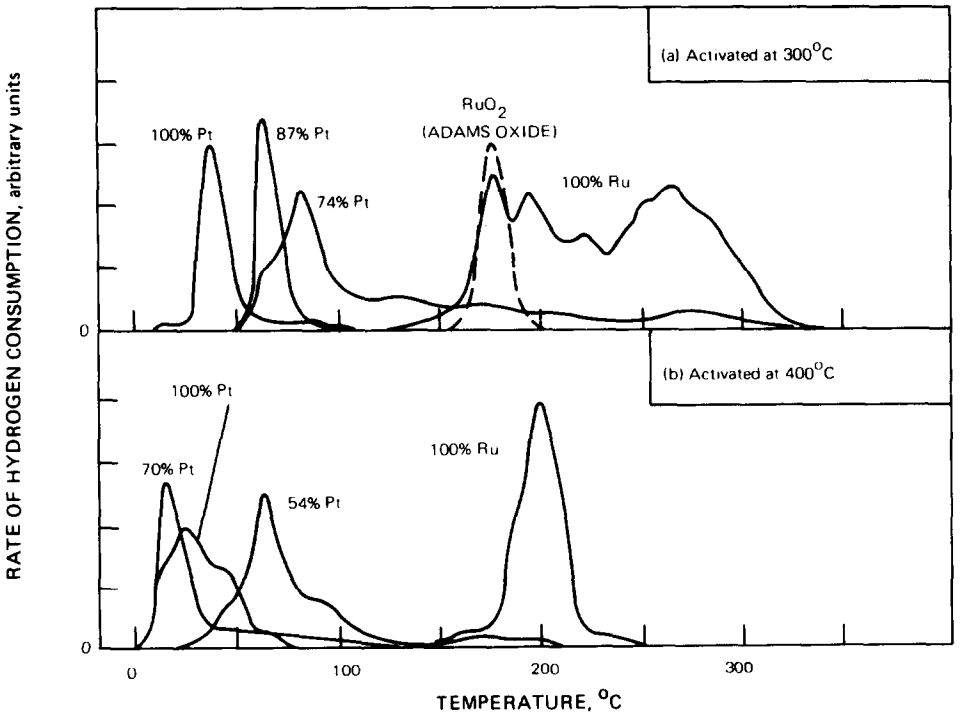

FIG. 5. TPR characteristics of Pt–Ru bimetallic catalysts supported on carbon fibre paper.

the monometallic cases in which ligand displacement in the impregnated metal complex by acidic surface groups assists alloy formation and subsequent dispersion of the activated catalyst. This work shows that the impregnation stage is an important step in the preparation of binary alloy catalysts of this type. Attempts to prepare well dispersed Pt–Ru catalysts, for example on γ-Al_2O_3 by Blanchard *et al.* (*38*), have partially failed owing to difficulties in preparing a homogeneous distribution of Pt and Ru at the impregnation stage.

The support also appears to influence the chemical nature of the dried mixture, as evidenced by differences in the total H_2 uptake listed in Table 1 and illustrated graphically in Fig. 7. From this figure it can be seen that increasing the Ru fraction in the unsupported case brings about a decline in the specific uptake of H_2 in contrast with the opposite behaviour for carbon-supported compounds. Evidently, in the absence of the carbon support evaporation of the impregnating solution results in a lower degree of substitution by nitrato-groups in the octahedral Ru complex, e.g., forming $[Ru(NO)(NO_3)(H_2O)_4]$ (*21*).

Activation of Pt–Ru bimetallic impregnated catalysts in air at 300°C produces very similar catalysts irrespective of the presence of a support. Both types of catalyst display a similar linear relationship between the temperature of the TPR maxima and bulk alloy composition (Fig. 6) and also between specific H_2 uptake and composition (Fig. 7). The form of the reduction peak for the Pt–Ru catalysts consists primarily of a single sharp peak indicative of alloy formation (*20*) superimposed on a lesser broadened background extending to higher temperatures attributed to a partially decomposed Ru component. Subsequent activation of Pt–Ru mixtures on PGCF paper at 400°C effectively eliminated the undecomposed fraction, yielding essentially simple reduction peaks during TPR (Fig. 5).

Thus TPR provides an average analysis

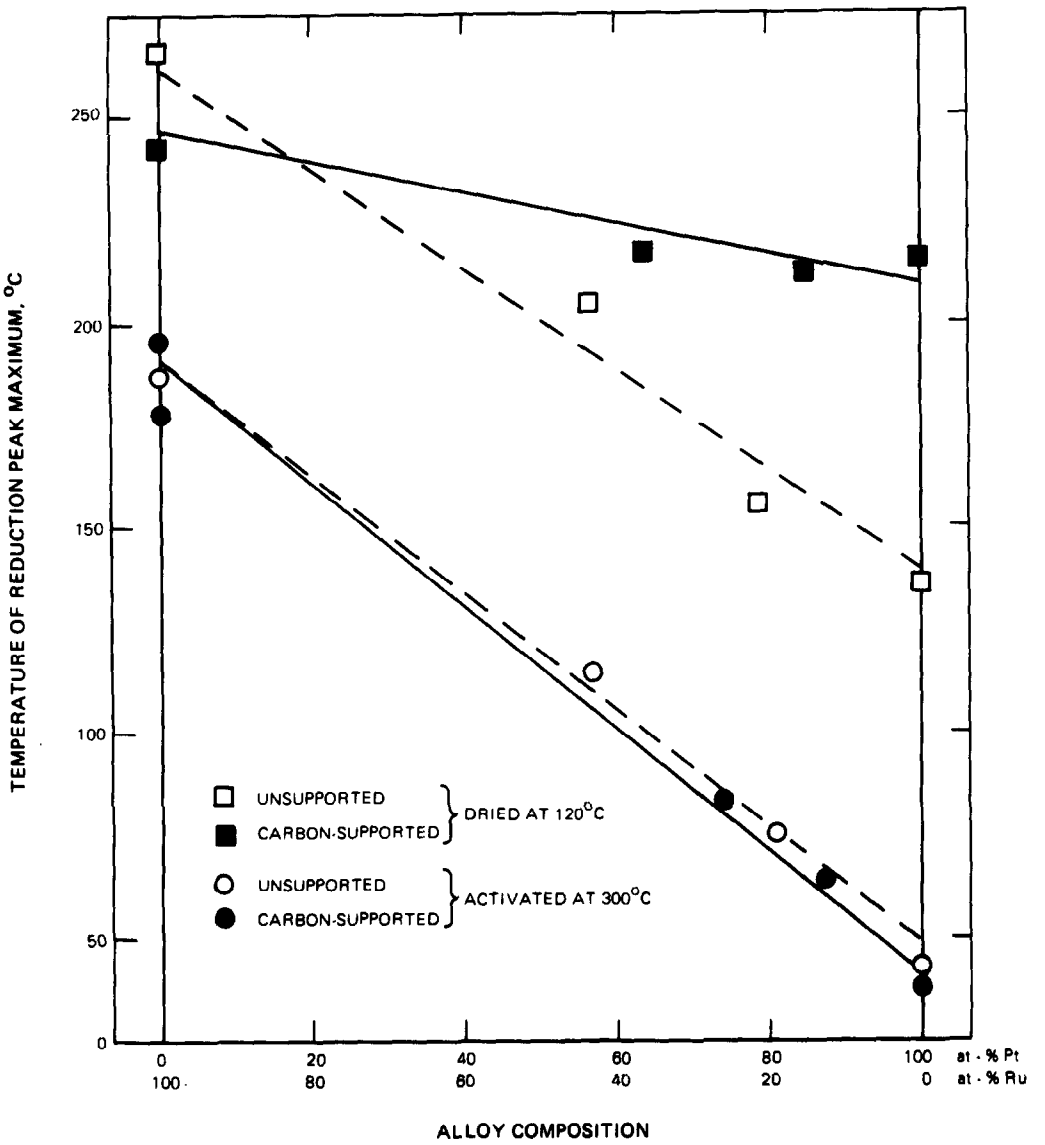

FIG. 6. Effect of bulk alloy composition and pretreatment on temperature of TPR maxima.

of the surface and bulk reducible species indicating the existence of an interaction between the carbon support and metal salts during impregnation from acidic media. This interaction serves to enhance the final metal dispersion, as determined electrochemically (see below). The technique also furnishes evidence for an alloy-type interaction in bimetallic Pt–Ru catalysts initially brought about during the impregnation/drying stage. On the other hand calcination at 300–400°C destroys the original interaction with the carbon support, whilst maintaining the alloyed nature of the catalyst.

Cyclic voltammetric studies of carbon-supported Pt–Ru catalysts were carried out on various samples activated at 300 and 400°C. Figures 8 and 9 illustrate the current–potential behaviour of catalysts activated at these two temperatures. As in the case of the monometallic Pt catalysts, an initial cathodic sweep at a relatively slow

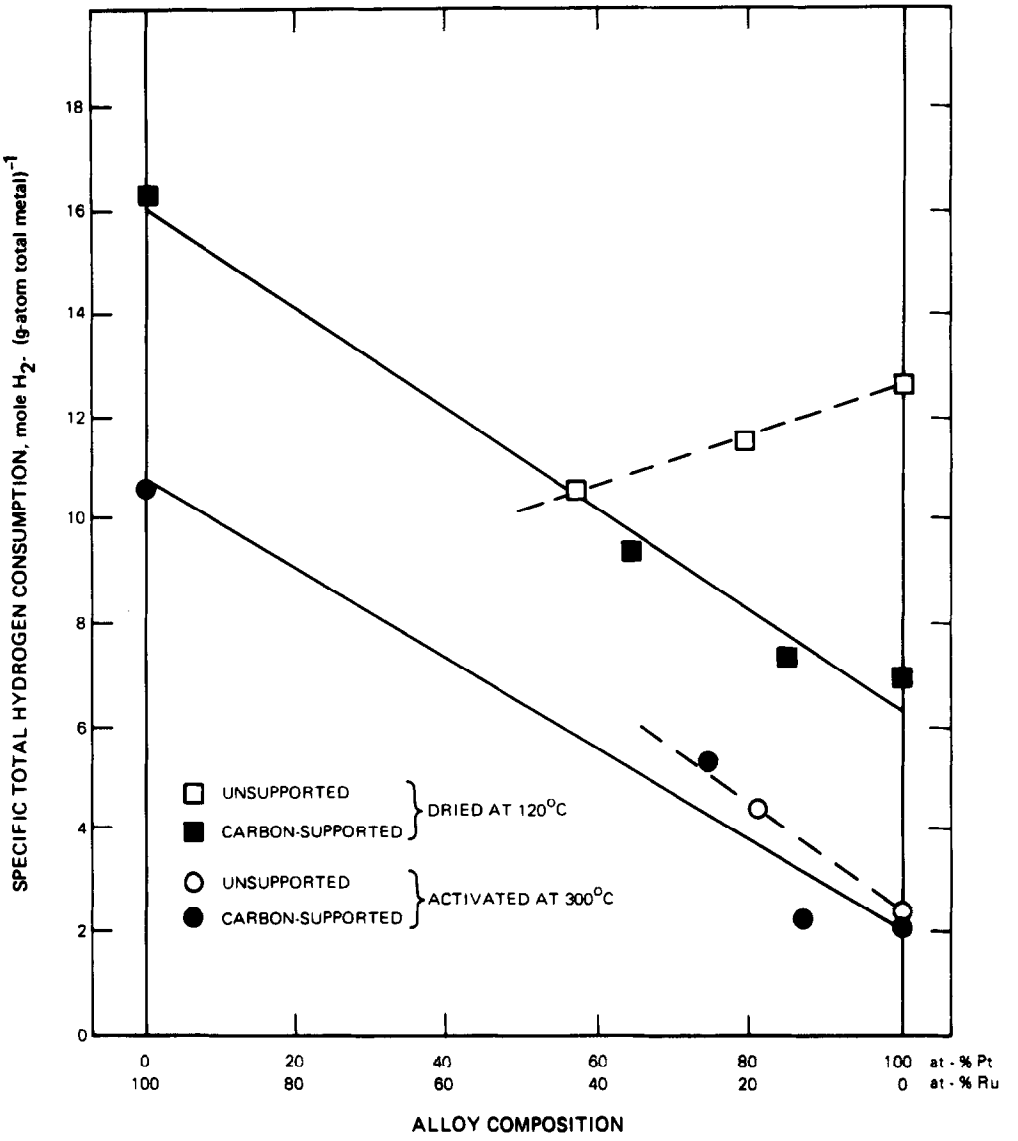

FIG. 7. Total hydrogen uptake during TPR of unsupported and supported Pt–Ru bimetallic catalysts.

rate of 2 mV sec^{-1} from the observed open-circuit potential, was carried out to characterise the oxide composition of the surface and subsurface regions. Activation at 300°C of a catalyst possessing a 72:28, Pt:Ru bulk composition leads to a near-surface component which reduces electrochemically in several stages. A broad reduction peak of low intensity extends initially from +0.8 to +0.4 V and consumes 16% of the total charge, q_{ox}. The remainder of the process takes place in two steps yielding narrow cathodic peaks at +0.148 and +0.101 V. Evidently, 300°C activation leads to a relatively inhomogeneous surface containing a number of reducible species. A subsequent potentiodynamic cycle of the fully reduced catalyst between 0.0 and +1.4 V revealed several anodic processes at potentials in excess of +1.1 V which subsequently reduced in at least four steps at 1.28, 1.20, 1.06, and 0.75 V during the cath-

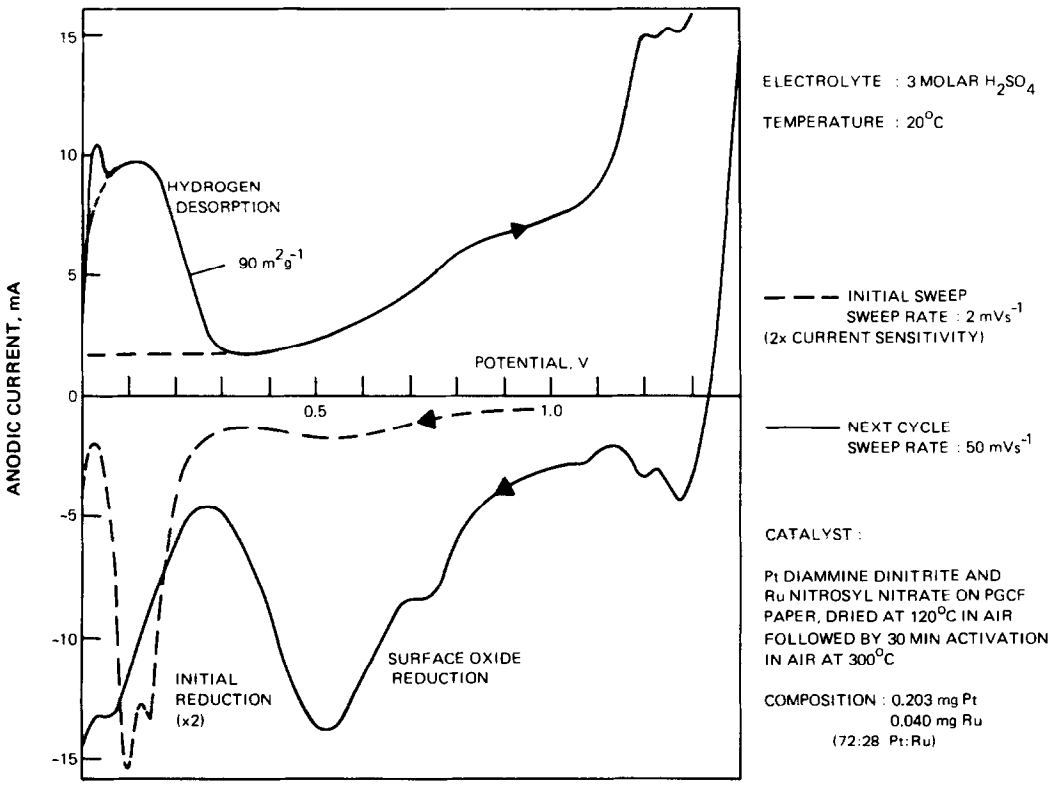

FIG. 8. Cyclic voltammogram of a bimetallic Pt–Ru catalyst supported on carbon fibre paper. Activated at 300°C.

odic sweep. Such behaviour is typical of Ru metal, which is able to form various surface oxides in the anodic potential region (*26*), e.g.

$$2Ru + 3H_2O = Ru_2O_3 + 6H^+ + 6e^-, \quad E^\circ = 0.74\ V, \quad (8)$$

$$Ru_2O_3 + H_2O = 2RuO_2 + 2H^+ + 2e^-, \quad E^\circ = 0.94\ V, \quad (9)$$

and

$$RuO_2 + 2H_2O = RuO_4 + 4H^+ + 4e^-, \quad E^\circ = 1.39\ V. \quad (10)$$

The cathodic peaks observed during the reverse sweep represent the corresponding reduction of these oxides forming either Ru metal or soluble Ru^{2+} species, e.g.

$$Ru_2O_3 + 6H^+ + 2e^- = 2Ru^{2+} + 3H_2O, \quad E^\circ = 1.30\ V, \quad (11)$$

and

$$RuO_2 + 4H^+ + 2e^- = Ru^{2+} + 2H_2O, \quad E^\circ = 1.12\ V. \quad (12)$$

Thus it is clear that a considerable proportion of unalloyed Ru is present after 300°C activation in air, probably originating from the partially decomposed Ru salt detected in TPR. The major reduction peak at +0.52 V in the reduced catalyst is characteristic of Pt–Ru Adams catalysts (*7*) and corresponds to reduction of a superficial alloyed oxide layer.

Although activation at 300°C in air yields a high bimetallic dispersion (90 $m^2\,g^{-1}$, (Fig. 8)), activation at 400°C results in more perfect alloy formation and consequently to an increased activity as an electrocatalyst for methanol electrooxidation at the expense of a reduced dispersion (54 $m^2\,g^{-1}$). Figure 10

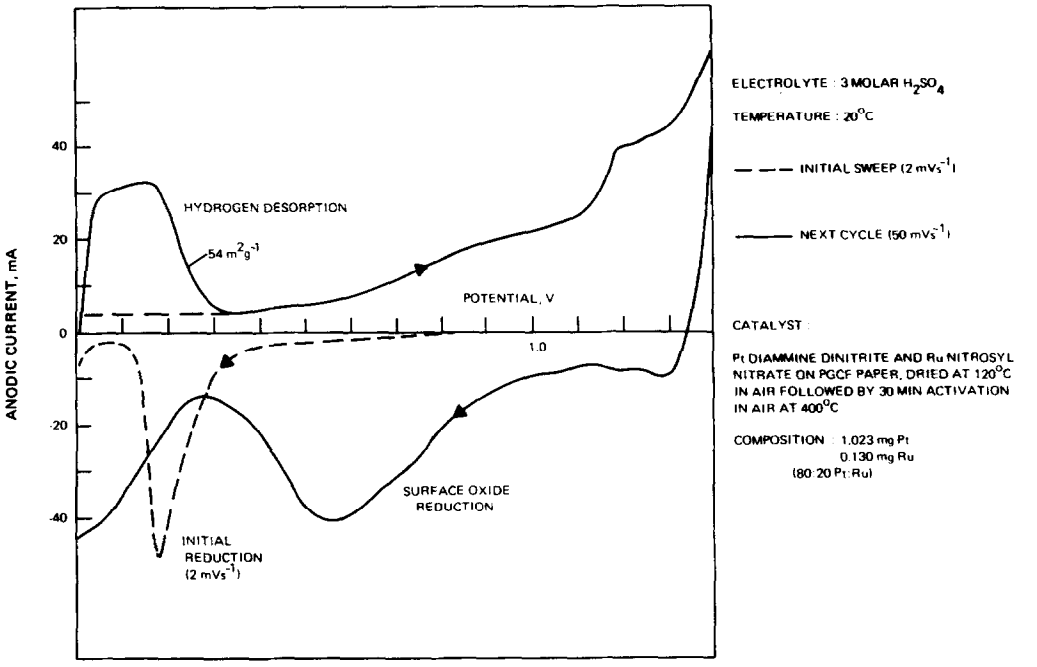

FIG. 9. Cyclic voltammogram of a bimetallic Pt–Ru catalyst supported on carbon fibre paper. Activated at 400°C.

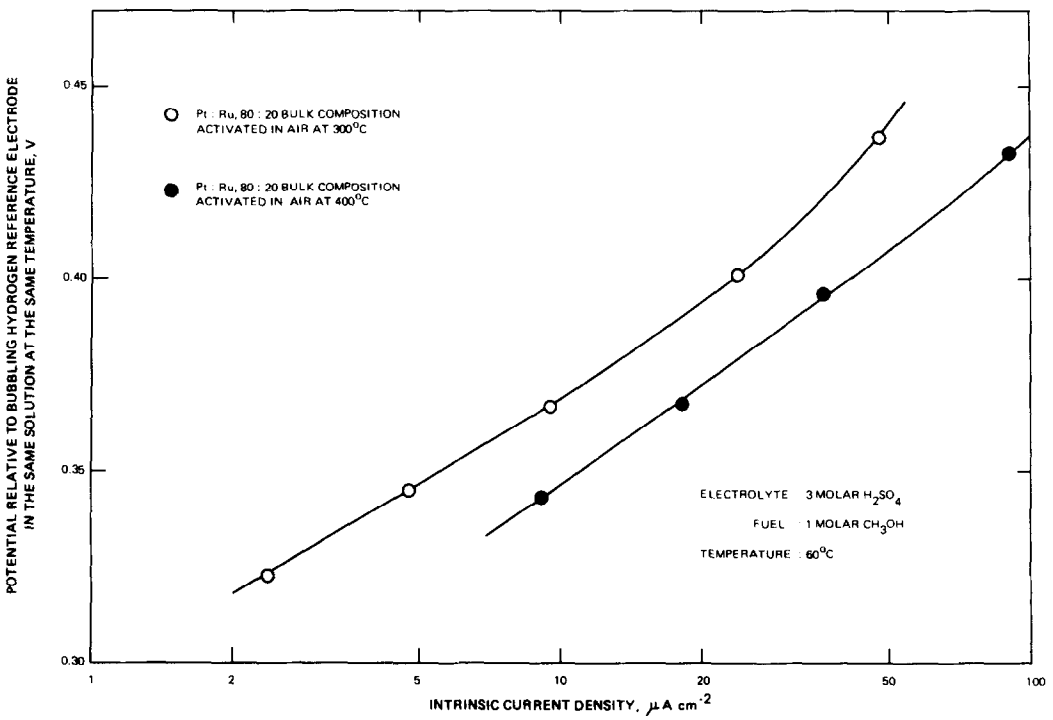

FIG. 10. Anodic oxidation of methanol on Pt–Ru alloy catalysts supported on pyrographite-coated carbon fibre paper.

shows Tafel plots of electrode potential against logarithmic current density per unit metal surface area for Pt–Ru catalysts, prepared by activation at 300 and at 400°C and possessing the same final bulk composition (80 : 20, Pt : Ru). Activities differ by a factor of approximately two at constant overpotential as measured in aqueous $3M$ H_2SO_4 containing $1M$ methanol at 60°C. The voltammogram of a catalyst activated at 400°C (Fig. 9) shows only a single reducible species during the initial linear cathodic sweep, supporting the TPR findings. Few traces of unalloyed Ru are found in the subsequent potentiodynamic cycle. Also Pt–Ru catalysts containing identical (80 : 20) bulk ratios of Pt and Ru show a significant anodic shift in the surface oxide reduction peak from 0.47 ± 0.02 to 0.57 V after activation at the higher temperature of 400°C. Generally we observe a uniform shift in the peak maximum, similar to that observed by Rand and Woods (*16*) for Pt–Rh alloys, from +0.40 to +0.75 V on going from highly dispersed catalysts containing approximately 50 at.% Ru to monometallic Pt catalysts. Hence the observed anodic shift in the surface oxide reduction peak after activation at 400°C is evidence of a lowering in surface enrichment by Ru, which normally occurs in mixed Pt–Ru catalysts after activation in air at 300°C (*7*).

On relating the coulombic charge associated with the initial intense reduction at ca. 0.1 V to the metal surface area we find, once again, that the equivalent of approximately 4 to 5 monolayers of PtO_2–RuO_2 are electrochemically reduced during the initial linear sweep. For such very highly dispersed catalysts this degree of reduction accounts for virtually the entire bulk of the sample.

CONCLUSIONS

We have illustrated the complementary nature of TPR and CV in characterising carbon-supported Pt and Pt–Ru catalysts. A substantial catalyst–support interaction is observed after the initial drying stage for catalysts prepared from HNO_3 solutions, which is attributed to the involvement of previously identified acidic surface oxide groups. For both monometallic and bimetallic catalysts the support interaction, though lost on activation in air at 300°C, assists in the formation of high metallic dispersions. For the Pt–Ru catalysts, activation in air at 300°C yields a high dispersion (ca. 90 $m^2\ g^{-1}$) whereas activation at 400°C results in more perfect alloy formation and consequently to an increased activity for methanol electrooxidation at the expense of a reduced dispersion (ca. 54 $m^2\ g^{-1}$). For air-activated catalysts the initial electrochemical reduction extends to approximately four monolayers irrespective of the particle size of the PtO_2 or PtO_2–RuO_2 oxides. Our electrochemical study appears to be the first reported for the reduction of dispersed oxides of platinum and the mechanistic conclusions appear to be generally similar (although different in detail) to published reports of the electrochemical reduction of anodically oxidised smooth platinum electrodes. Further details concerning the electrochemical reduction of such dispersed oxide particles are to be published elsewhere.

REFERENCES

1. van den Berg, G. H., and Rijnten, H. Th., *in* "Preparation of Catalysts II" (B. Delmon, P. Grange, P. Jacobs, and G. Poncelet, Eds.), p. 265. Elsevier, Amsterdam, 1979.
2. Berrebi G., and Bernusset, Ph., *in* "Preparation of Catalysts I" (B. Delmon, P. Jacobs and G. Poncelet, Eds.) p. 13. Elsevier, Amsterdam, 1976.
3. Sinfelt, J. H., and Cusumano, J. A., *in* "Advanced Materials in Catalysis" (J. J. Burton and R. L. Garten, Eds.), p. 1. Academic Press, New York, 1977.
4. Anderson, J. R., "Structure of Metallic Catalysts," p. 163. Academic Press, New York, 1975.
5. Seah, M. P., and Lea, C., *Philos. Mag.*, **31**, 627 (1975).
6. Sachtler, W. M. H., and van Santen, R. A., *Appl. Surf. Sci.* **3**, 121 (1979).
7. McNicol, B. D., and Short, R. T., *J. Electroanal. Chem.* **81**, 249 (1977).
8. Jenkins, J. W., McNicol, B. D., and Robertson, S. D., *Chem. Technol.* **7**, 316 (1977).

9. Robertson, S. D., McNicol, B. D., de Baas, J. H., Kloet, S. C., and Jenkins, J. W., *J. Catal.* **37**, 424 (1975).
10. Wagstaff, N., and Prins, R., *J. Catal.* **59**, 434 (1979).
11. Yao, H. C., and Shelef, M., *J. Catal.* **44**, 392 (1976).
12. Yao, H. C., Japar, S., and Shelef, M., *J. Catal.* **50**, 407 (1977).
13. Bolivar, C., Charcosset, H., Frety, R., Primet, M., Tournayan, L., Betizeau, C., Leclercq, G., and Maurel, R., *J. Catal.* **39**, 249 (1975).
14. Nicholson, R. S., *Anal. Chem.* **37**(11), 1351 (1965).
15. Wopschall, R. H., and Shain, I., *Anal. Chem.* **39**(13), 1514 (1967).
16. Rand, D. A. J., and Woods, R., *J. Electroanal. Chem.* **36**, 57 (1972).
17. Mayell, J. S., and Barber, W. A., *J. Electrochem. Soc.* **116**, 1333 (1969).
18. Connolly, J. F., Flannery, R. J., and Aronowitz, G., *J. Electrochem. Soc.* **113**, 577 (1966).
19. Kinoshita, K., Lundquist, J., and Stonehart, P., *J. Catal* **31**, 325 (1973).
20. McNicol, B. D., and Short, R. T., *J. Electroanal. Chem.* **92**, 115 (1978).
21. Lowde, D. R., Williams, J. O., Attwood, P. A., Bird, R. J., McNicol, B. D., and Short, R. T., *J. Chem. Soc. Faraday Trans. I* **75**, 2312 (1979).
22. Attwood, P. A., McNicol, B. D., and Short, R. T., *J. Catal.* **67**, 287 (1981).
23. Brummer, S. B., *J. Phys. Chem.* **69**, 562 (1965).
24. Biegler, T., Rand, D. A. J., and Woods, R., *J. Electroanal. Chem.* **29**, 269 (1971).
25. Mellor, J. W., "A Comprehensive Treatise on Inorganic and Theoretical Chemistry," Vol. 8, p. 515. Longmans, Green, London, 1940.
26. Milazzo, G., and Caroli, S., "Tables of Standard Electrode Potentials." Wiley, New York/London, 1978.
27. Anson, F. C., and Lingane, J. J., *J. Amer. Chem. Soc.* **79**, 4901 (1957).
28. Shibata, S., and Sumino, M. P., *Electrochim. Acta* **16**, 1089 (1971).
29. Shibata, S., *Electrochim. Acta* **17**, 395 (1972).
30. Shibata, S., *J. Electroanal Chem.* **89**, 37 (1978).
31. Shibata, S., and Sumino, M. P., *J. Electroanal. Chem.* **99**, 187 (1979).
32. Gileadi, E., Fullenwider, M. A., and Bockris, J. O'M., *J. Electrochem. Soc.* **113**, 926 (1966).
33. Angerstein-Kozlowska, H., Conway, B. E., Barnett, B., and Mozota, J., *J. Electroanal. Chem.* **100**, 417 (1979).
34. Fletcher, J. M., Jenkins, I. L., Lever, F. M., Martin, F. S., Powell, A. R., and Todd, R., *J. Inorg. Nucl. Chem.* **1**, 378 (1955).
35. Fletcher, J. M., Brown, P. G. M., Gardner, E. R., Hardy, C. J., Wain, A. G., and Woodhead, J. L., *J. Inorg. Nucl. Chem.* **12**, 154 (1959).
36. Fletcher, J. M., and Woodhead, J. L., *J. Inorg. Nucl. Chem.* **27**, 1517 (1965).
37. Maya, L., *J. Inorg. Nucl. Chem.* **41**, 67 (1979).
38. Blanchard, G., Charcosset, H., Chenebaux, M. T., and Primet, M., *in* "Preparation of Catalysts II" (B. Delmon, P. Grange, P. Jacobs, and G. Poncelet, Eds.), p. 197. Elsevier, Amsterdam, 1979.